Experimental and theoretical scaling laws for transverse diffusive broadening in two-phase laminar flows in microchannels

Cite as: Appl. Phys. Lett. **76**, 2376 (2000); https://doi.org/10.1063/1.126351
Submitted: 29 October 1999 • Accepted: 24 February 2000 • Published Online: 18 April 2000

Rustem F. Ismagilov, Abraham D. Stroock, Paul J. A. Kenis, et al.

Experimental and theoretical scaling laws for transverse diffusive broadening in two-phase laminar flows in microchannels

Rustem F. Ismagilov, Abraham D. Stroock, Paul J. A. Kenis, and George Whitesides[a),b)]
Department of Chemistry and Chemical Biology, Harvard University, Cambridge, Massachusetts 02138

Howard A. Stone[a),c)]
Division of Engineering and Applied Sciences, Harvard University, Cambridge, MA 02138

(Received 29 October 1999; accepted for publication 24 February 2000)

This letter quantifies both experimentally and theoretically the diffusion of low-molecular-weight species across the interface between two aqueous solutions in pressure-driven laminar flow in microchannels at high Péclet numbers. Confocal fluorescent microscopy was used to visualize a fluorescent product formed by reaction between chemical species carried separately by the two solutions. At steady state, the width of the reaction–diffusion zone at the interface adjacent to the wall of the channel and transverse to the direction of flow scales as the one-third power of both the axial distance down the channel (from the point where the two streams join) and the average velocity of the flow, instead of the more familiar one-half power scaling which was measured in the middle of the channel. A quantitative description of reaction–diffusion processes near the walls of the channel, such as described in this letter, is required for the rational use of laminar flows for performing spatially resolved surface chemistry and biology inside microchannels and for understanding three-dimensional features of mass transport in shearing flows near surfaces. © *2000 American Institute of Physics.* [S0003-6951(00)02616-4]

Chemical patterning at the interface of two miscible fluids flowing laminarly and in parallel provides a method of microfabrication: examples include fabrication of microelectrodes[1] and patterning of mammalian and microbial cells.[2] The rational use of laminar flow for patterning and fabrication inside microchannels requires an improved understanding of the convective–diffusive transport processes near the walls of the channel. The most relevant component of this transport occurs across the interface between the flowing solutions *transverse* to the direction of the flow. In this letter, we combine experiments and theory to quantify this transverse diffusive transport as a function of the local flow speed and velocity profile.

Pressure-driven flow in microchannels generally is laminar, since the Reynolds numbers Re are small (under 100). Laminar flow patterning occurs by a chemical reaction at the interface between two miscible fluids flowing through a channel.[1] Here, we use confocal fluorescent microscopy to visualize the fluorescent product of the reaction between two nonfluorescent chemical species carried separately by the two flowing solution streams. The spatial extent of transverse diffusive mixing can be decreased by increasing the average flow speed (so long as the Reynolds number is small enough that the flow is laminar). We demonstrate experimentally that, at steady state near the top and bottom walls of the channel, the extent of transverse diffusive mixing across the fluid–fluid interface scales as the one-third power of the axial distance (z) along the channel and scales inversely as the one-third power of the maximum flow velocity. The extent of such mixing near the middle of the channel, where the flow speed is nearly uniform, scales as the more familiar one-half power of the axial distance (z) along the channel and inversely as the one-half power of the average flow velocity. Theoretical arguments are given for these two different scaling laws.

To test the predictions of the theory, we have fabricated microfluidic channels using the ''rapid prototyping'' technique described previously,[3] and used a single syringe pump to drive the fluids into the two inlets at a constant flow rate. Rather than deducing the extent of diffusive mixing from the flow profiles, we chose a direct approach—visualization of the region of diffusive mixing using confocal fluorescent microscopy (Leica TCS). Fluo-3 (m.w.=770; we used the pentaammonium salt) is a commercially available, nonfluorescent compound that forms a strongly fluorescent 1:1 complex with a calcium ion ($K_d = 0.39\ \mu$M).[4] The formation of the complex is diffusion controlled, therefore, we could visualize the region of diffusive mixing by observing the concentration of this complex near the interface between flowing aqueous solutions (pH$\approx$6.5) of 5 μM fluo-3 and 1 mM $CaCl_2$ (Fig. 1). All experiments were conducted at room temperature, and it took 2–4 s to acquire each image in the line-averaging mode. At a given axial distance z from the point where the streams join, the diffusive mixing is more extensive (i.e., the fluorescent region is broader) in the slower-moving fluid near the wall of the channel than in the middle of the channel. At low flow velocities we observe some interdiffusion in the dead volume of the Y junction [Fig. 1(b)], and we assume that its effect on the scaling behavior is negligible.[5] Below, we argue that the transverse diffusive broadening—which, ideally, should be limited in chemical patterning applications—obeys power-law behavior as a function of distance along the channel z and the average flow speed U_a.

In order to quantify the scaling relationships that describe diffusive mixing in the laminar flows present in our experiments, we use the convective–diffusion equation for

a)Authors to whom correspondence should be addressed.
b)Electronic mail: gwhitesides@gmwgroup.harvard.edu
c)Electronic mail: has@stokes.deas.harvard.edu

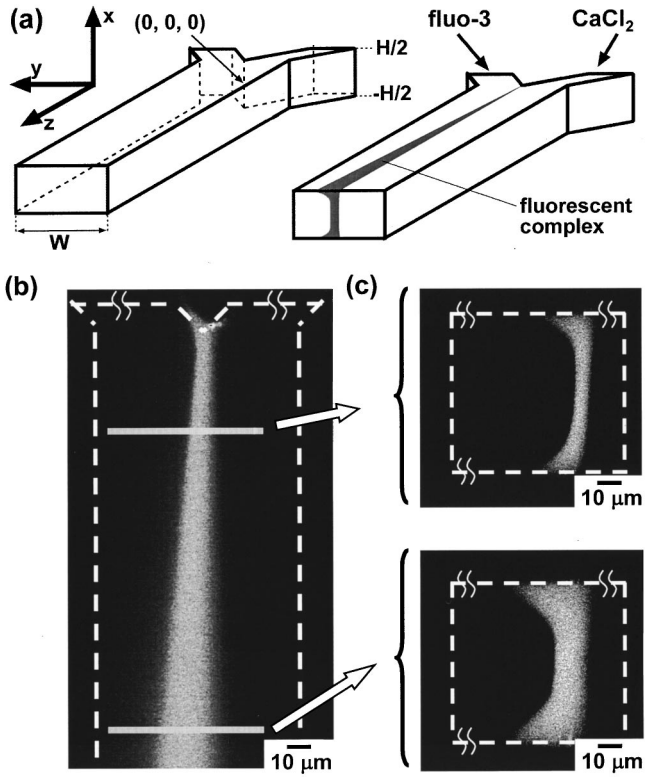

FIG. 1. (a) Schematic drawing of the experiment used to generate fluorescence in the microchannel, and the coordinate system employed. The dashed lines indicate the internal edges of the channel. H is the height of the channel. The origin of the coordinate system is located in the middle of the vertical edge shared by both channels in the Y junction. (b) and (c) Data obtained for the fluo-3/Ca^{2+} system by confocal fluorescence microscopy in: (b) A 100×250 μm^2 yz slice obtained 12 μm from the top of the channel (average velocity of the flow $U_a=0.7$ cm/s, Re=0.4; the Reynolds number $\mathrm{Re}=\rho U_a H/\mu$, where ρ is the density of the solutions and μ is the viscosity). Some mixing is visible in the area of the dead volume of the Y junction. (c) Corresponding 90×90 μm^2 cross sections in the xy plane of the channel obtained 50 μm (top) and 200 μm (bottom) from the Y junction.

steady-state transport of chemical species, with concentration $c(x,y,z)$, in the flow field $\mathbf{u}(x,y,z)$, with velocities scaled by the average flow speed U_a and lengths scaled by the channel height H,

$$P\mathbf{u}\cdot\nabla c=\nabla^2 c\cong\left(\frac{\partial^2}{\partial x^2}+\frac{\partial^2}{\partial y^2}\right)c \tag{1}$$

[the coordinate system employed is shown in Fig. 1(a)]. Here, D is the diffusion coefficient, and P is the dimensionless Péclet number, $P=U_aH/D$, which compares the typical time scale for diffusive transport to that for convective transport in a channel with a given height H. P is large in our experiments (for $H=6\times10^{-5}$ m, $D=10^{-9}$ m^2/s, $U_a=0.0025-0.5$ m/s, $P=150-30\,000$). Therefore, in Eq. (1) we neglect diffusive transport along the flow (z) direction.

If the transverse diffusive broadening $\delta(z)$ is monitored as a function of distance z down the channel, then the comparison of the high Péclet number to the ratio z/H distinguishes two regimes. For $P\gg z/H\gg1$ (our experiments are in this regime), the diffusive broadening $\delta(z)$ also depends on x [as proposed by Kamholz *et al.*[6] and shown in Fig. 1(c) here] because the nonuniform velocity profile affects the diffusion process. For $z/H\gg P\gg1$, $\delta(z)$ is approximately independent of x because diffusive transport on the scale H eliminates the effects of the nonuniform velocity profile. Kamholz *et al.* analyzed their data assuming the latter regime, and their experiments were indeed conducted at lower $P/(z/H)$ ratios.[6] In this respect, the two approaches are complimentary to each other.

In the present study, the velocity field is the uniaxial Poiseuille-like flow (in a rectangular channel with width W and height H), which, although known in the form of a Fourier series, is sufficiently complicated that no simple analytical solution can be obtained to Eq. (1).

Instead of obtaining a numerical solution, we indicate two scaling laws for transverse diffusion that are natural consequences of Eq. (1) for channel flow. We utilize the fact that the flow profile at the interface ($y=0$) is approximately parabolic in x, with a maximum velocity in the middle of the channel ($x=0$), and with zero velocity at the walls ($x=\pm H/2$). Near the middle of the channel—where $[(x/(H/2)]^2\ll1$ and $[y/(W/2)]^m\ll1$, $m\sim4$ for our channels[7]—the velocity is nearly uniform and approximately equal to the maximum velocity $U_m(\approx2U_a)$. Also, near the top and bottom boundaries, $\tilde{x}^2\ll1$ and $[y/(W/2)]^m\ll1$, where $\tilde{x}=H/2-|x|$, the velocity is approximately a linear function of the x-position, $\mathbf{u}(x,y,z)=G\tilde{x}\mathbf{e}_z$. The shear rate, $G\ (s^{-1})\approx8(U_a/H)$, and $\mathbf{e}_z$ is the unit vector along the axis of the channel. It is this linear variation of velocity (that increases from zero at the solid boundary) that gives rise to the one-third power law for transverse diffusion near the walls of the channel. Near the center of the channel, $\mathbf{u}=U_m\mathbf{e}_z+O([x/(H/2)]^2)$, so we can rewrite Eq. (1) in dimensional form $U_m\partial c/\partial z=D\nabla^2 c$. Thus, in the center of the channel, the transverse mass transport is simple diffusion, and by dimensional reasoning, this equation implies that an initial concentration distribution broadens in x and y as a function of the z position according to $\delta(z)\propto(Dz/U_a)^{1/2}$. We defined the thickness $\delta(z)$ of the interfacial diffusion layer as the distance over which the concentration of the fluorescent complex falls to 0.2 of its maximum value.

A special case of transverse diffusion in the linear flow near a fixed boundary is known as the Lévêque problem.[8] This problem treats diffusion perpendicular to the boundary (along $\mathbf{e}_x$) and across a linear flow field, $\mathbf{u}=G\tilde{x}\mathbf{e}_z+O([\tilde{x}/(H/2)]^2)$. We will extend this classical result to account for diffusion in the other transverse direction, $\mathbf{e}_y$. In the traditional two-dimensional Lévêque problem, the approximate form of Eq. (1) for high-Péclet-number flow with $\partial c/\partial y=0$ is $G\tilde{x}\partial c/\partial z=D\,\partial^2 c/\partial\tilde{x}^2$. Hence, diffusive transport in x will depend on the distance down the channel z as $\delta(z)\propto(Dz/G)^{1/3}\propto(DHz/U_a)^{1/3}$.

We must now relate this standard Lévêque result for the diffusive transport along $\mathbf{e}_x$ to the diffusive transport along $\mathbf{e}_y$, as it is this (transverse) variation that leads to mixing and to the subsequent chemical reaction of the species present in the two adjacent laminar flows in our experiments. To do this, we rewrite Eq. (1) in cylindrical coordinates with the dimensionless similarity variable $\eta=r/(Dz/G)^{1/3}$. Here, $\tilde{x}=r\cos\theta$ and $y=r\sin\theta$ for $-\pi<2\theta<\pi$ and $C(\eta,\theta)=c(\nu,\theta,z)$:

$$-\frac{\eta^2\cos\theta}{3}\left(\frac{\partial C}{\partial\eta}\right)=\frac{1}{\eta}\frac{\partial}{\partial\eta}\left(\eta\frac{\partial C}{\partial\eta}\right)+\frac{1}{\eta^2}\frac{\partial^2 C}{\partial\theta^2}. \tag{2}$$

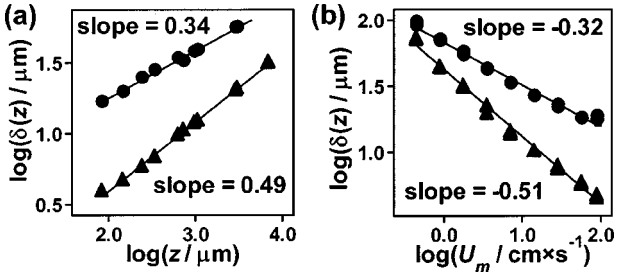

FIG. 2. Plot of the width of the region mixed by diffusion δ as a function of (a) the axial distance z from the Y junction ($H=105\mu$m) and (b) the average velocity of the flow U_a, calculated from the volumetric flow rate (μL/min) and the cross-sectional area of the channel ($H=55\mu$m). The size of the symbols corresponds approximately to the error in the determination of the values that the symbols represent. Lines show the linear regression fits to the data. In the middle of the channel (▲) the mixed region broadens as the 1/2 power of both z and U_a; near the wall (●) the mixed region broadens as the 1/3 power of the ratio of z and U_a^{-1}. The data for (a) were collected at $U_a=8$ cm/s, Re=8.4. The data for (b) were collected 500 μm from the Y junction, with U_a ranging from 0.23 to 46 cm/s, and Re ranging from 0.13 to 26.

Equation (2) has no free parameters associated with it. An analytical solution to this equation subject to appropriate boundary conditions appears to be complicated. Nevertheless, we conclude that all variations in $C(\eta,\theta)$ will occur on a scale of order one in η. This conclusion implies that, in terms of the original variables, $c(r,\theta,z)$ will vary in both transverse directions (x and y) on the scale $\delta\sim r\propto(Dz/G)^{1/3}\propto(DHz/U_a)^{1/3}$.

To test the theoretical predictions, we analyzed experimental data with SCION IMAGE.[9] For a given x (on each image we analyzed images only near $x\approx 0$ and near $x\approx H/2$) the width $\delta(z)$ of the region mixed by diffusion was taken to be the width of the fluorescent region with the intensity above 0.2 of the maximum intensity. The spreading $\delta(z)$ was always sufficiently small to be in a flow with uniform velocity profile in the y direction.

The experimental data confirmed the theoretical predictions. Near the wall of the channel, the width of the region mixed by diffusion scales as the 1/3 power (0.33 ± 0.02) of the ratio of the axial distance z [Fig. 2(a)] and the average velocity of the fluid U_a [Fig. 2(b)]. For the uniform flow regime in the middle of the channel, we observed the expected square root (0.5 ± 0.02) dependence on the ratio of z and U_a.

Our theoretical analysis predicts two effects of decreasing the channel height H while keeping other parameters constant. First, it decreases the Péclet number and makes the difference between the diffusion near the top and bottom walls and in the center in the channel less dramatic, and in the limiting case the nonuniformity of diffusion can be ignored.[6] Second, in the high-Péclet-number limit it decreases the extent of the diffusional broadening $\delta\sim(DHz/U_a)^{1/3}$ near the top and bottom walls.

Even though the scaling laws by themselves are not sufficient for designing devices with specific characteristics, the results presented in this letter provide a basis for the rational control of spatially resolved transport processes at interfaces between phases in pressure-driven laminar flows. For example, understanding the scaling behavior of transverse diffusion near the surface of the channel is required for predicting the resolution of patterning and fabrication with laminar flow,[1] for the design of ''diffusional T sensors,''[10,11] passive mixers, and other components for micrototal analysis systems.[12] The experimental technique described in this letter captures both the diffusive and convective transport processes within the fluid, and we believe that it will be broadly applicable to the imaging of more complex fluid flows, and to visualization of other technologically important transport problems such as mixing. The extension of the scaling arguments from the Lévêque problem to molecular lateral diffusion near the wall of a channel that we have validated experimentally should be applicable to the description of other diffusion-like phenomena such as heat and mass transfer, which influence many chemical and biological systems.[13] This extension is particularly important for adequate design of sensors operating in flows with linear shear, especially sensors in microchannels.[14]

This work was supported by DARPA, NSF ECS-9729405 [for one of the authors (G.M.W.)]; by DARPA Army Research Office DAAG55-97-1-0114 [for one of the authors (H.A.S.)], and by the NSF MRSEC DMR-9809363 [for two of the authors (G.M.W. and H.A.S.)]. One of the authors (A.D.S.) was supported by NIH Molecular Biophysical Training Grant No. 5T32GM08313-10. The authors acknowledge Shuichi Takayama for helpful suggestions.

[1] P. J. A. Kenis, R. F. Ismagilov, and G. M. Whitesides, Science **284**, 83 (1999).
[2] S. Takayama, J. C. McDonald, E. Ostuni, M. N. Liang, P. J. A. Kenis, R. F. Ismagilov, and G. M. Whitesides, Proc. Natl. Acad. Sci. USA **96**, 5545 (1999).
[3] D. C. Duffy, J. C. McDonald, O. J. A. Schueller, and G. M. Whitesides, Anal. Chem. **70**, 4974 (1998).
[4] Molecular Probes, 4849 Pitchford Ave., Eugene, OR 97402-9165; internet address: http://www.molecularprobes.com/
[5] There is also a pronounced asymmetry in the diffusion profile, partly because Ca^{2+} has a higher diffusivity ($D=1.2\times10^{-9}$ m^2/s) than fluo-3 ($D\approx10^{-10}$ m^{2}s). We do not know the coefficient of diffusion for fluo-3, and approximated it with the value for a similar dye Indo-1; L. A. Blatter and W. G. Wier, Biophys. J. **58**, 1491 (1990). The high initial concentration of Ca^2 (1 mM) relative to that of fluo-3 (5 μM) makes our fluorescence measurement much more sensitive to diffusion of Ca^{2+}than to that of fluo-3, and increases the asymmetry of the diffusion profile. We added EDTA (4 μM) to the solution of fluo-3 in order to reduce the background fluorescence and increase contrast by scavenging opportunistic metal ions that could bind to fluo-3.
[6] A. E. Kamholz, B. H. Weigl, B. A. Finlayson, P. Yager, Anal. Chem. **71**, 5340 (1999); from the data provided we calculated for AB580 $P\approx$33-330, for HAS $P\approx1700$, and $z/H=200$.
[7] The parabolic flow profile in a rectangular channel with $W/H>2$ can be approximated with the following form: $u(x,y)=U_m(\{1-[x/(H/2)]^2\}\{1-[y/(W/2)]^m\})$, where $m=2.37-6.6$ for $W/H=2-5$.; from R. K. Shah, *Laminar Flow Forced Convection in Ducts* (Academic, New York, 1978), p. 197.
[8] M. A. Lévêque, Ann. Mines **13**, 201 (1928); H. A. Stone, Phys. Fluids **1**, 1112 (1989).
[9] We applied a 3×3 convolution smoothing routine five times to each image—the value to each pixel was replaced by the weighted averaged of its value (weighted by 4) with that of its eight nearest neighbors (weighted by 1).
[10] B. H. Weigl and P. Yager, Science **283**, 346 (1999).
[11] L. Pollack, M. W. Tate, N. C. Darnton, J. B. Knight, S. M. Gruner, W. A. Eaton, and R. H. Austin, Proc. Natl. Acad. Sci. USA **96**, 10115 (1999).
[12] W. Ehrfeld, L. J. Kricka, and H. Lehr, Top. Curr. Chem. **194**, 233 (1998); G. Blankenstein and U. D. Larsen, Biosens. Bioelectron. **13**, 427 (1998).
[13] S. Vogel, *Life in Moving Fluids* (Princeton University Press, Princeton, NJ, 1996).
[14] C. G. Phillips, Q. J. Mech. Appl. Math. **43**, 135 (1990); W. Zhang, H. A. Stone, and J. D. Sherwood, J. Phys. Chem. **100**, 9462 (1996).